COMMUNICATION

Check for updates

Mass spectrometry friendly pH-gradient anion exchange chromatography for the separation of full and empty adeno-associated virus (AAV) capsids†

Felipe Guapo, [iD] ‡[a] Florian Füssl,‡[a] Lisa Strasser[a] and Jonathan Bones [iD] *[ab]

The proportion of full and empty capsids represents a critical quality attribute of adeno-associated virus (AAV)-based therapeutics. In this study, pH-gradient anion exchange chromatography was utilized for the separation of full and empty capsid species. The developed method allowed for applicability to multiple AAV serotypes and facilitated subsequent mass spectrometric detection of intact AAVs. This is the first study demonstrating generic applicability as well as mass spectrometric compatibility, allowing for a more sophisticated analysis of AAV-based gene therapy and paving the way for future developments in the field.

Adeno-associated virus (AAV) has become a widely popular vector for therapeutic gene delivery.[1–3] Twelve AAV serotypes, which are well characterized in terms of tissue tropism and transduction efficiency, allow for directed administration into target tissue.[4] AAVs are composed of a capsid, which is assembled through multiple copies of three viral capsid proteins (VP1, 2 and 3) and equipped with single stranded DNA as transgene, which is meant for delivery into patient cells.[5] During production, impurities can emerge which lack the desired therapeutic properties. A common impurity which can account for more than 98% of the total of particles produced are capsids that have failed to package the gene of interest, rendering them therapeutically incompetent.[6,7] While in some scenarios these by-products can attract anti-AAV antibodies, thus acting as decoys, their presence inevitably necessitates the administration of higher doses of preparations to achieve a desired

therapeutic effect, fuelling the risk of dose-dependent immunogenic and cytotoxic responses.[8,9] In consequence, AAVs require characterization after production and before patient treatment to allow for evaluation and adjustment of the final particle composition. Despite being time consuming and requiring relatively large amounts of material, analytical ultra-centrifugation (AUC) is still considered the gold standard for the characterization of the AAV particle composition.[10] An alternative approach that has gained attention in recent years is anion exchange chromatography (AEX). The basis for separation in AEX is a difference in the isoelectric point (pI) of full and empty capsids of reportedly 0.4 units governed by the presence or absence of DNA.[11] This difference causes stronger retention of the more negatively charged full species on the AEX phase and later elution. Commonly, AEX is performed with a gradient of increasing ionic strength of up to several 100 mM and often non-linear gradients containing isocratic holds to achieve elution and separation.[12–17] While the isoelectric points of different AAV serotypes are in a similar region of around 6.3, they tend to behave differently on AEX separation phases, usually complicating the development of generically applicable methods and gradients.[11] Another bottleneck is the inability to differentiate other impurities such as partially filled particles.[18] The successful analysis of these forms was previously described through AUC, mass photometry and charge-detection mass spectrometry (CDMS).[19–23] In this contribution, we aimed to develop an AEX-based separation strategy that can overcome the above discussed limitations, *i.e.*, being generically applicable and mass spectrometry friendly. AEX chromatography was performed using a non-porous 3 μm particle column with highly monodisperse packing properties, facilitating the separation of large biomolecules with minimal Eddy-diffusion and good mass transfer, which generated sharp peaks, high chromatographic resolution and high sensitivity. Ion exchange chromatography can either rely on salt-gradient elution, pH-gradient elution, or a mixture thereof. Recent literature demonstrates that either mode can facilitate highly efficient separations of proteins and their isoforms.[24] While salt gradient

[a]*Characterisation and Comparability Laboratory, NIBRT – The National Institute for Bioprocessing Research and Training, Foster Avenue, Mount Merrion, Blackrock, Co. Dublin, A94 X099, Ireland. E-mail: jonathan.bones@nibrt.ie; Tel: +353 1215 8100. Fax: +353 1215 8116*

[b]*School of Chemical Engineering and Bioprocessing, University College of Dublin, Belfield, Dublin 4, D04 V1W8, Ireland*

† Electronic supplementary information (ESI) available: Experimental details; proportions of full and empty capsids in AAV sample mixtures; run-to-run comparison based on the AAV6 full/empty mixture. See DOI: https://doi.org/10.1039/d3ay01560b

‡ Authors contributed equally.

elution requires the use of a high ionic strength mobile phase, pH-gradient elution does not, which is clearly favourable when subsequent mass spectrometric interfacing is desired.[25,26] It was also shown that MS-friendly mobile phases of low ionic strength can outperform conventional non-volatile salt or pH-gradient separation systems in terms of separation performance, hence, in this study we further expanded our use of pH-gradient elution for complex biomolecule separation.[24] Mobile phases were developed that cover a wide pH-range to ensure sufficient binding and elution of AAV5, 6 and 8, which were investigated in this study.

Separation of full/empty mixtures of the three serotypes after gradient optimization are shown in Fig. 1. Notably, all serotypes were analyzed using the same gradient, suggesting that the chromatographic conditions might also be applicable to other serotypes, albeit these were not investigated due to material non-availability. All three AAVs elute late in the gradient which is primarily caused by the high pH at the gradient start, equivalent to a mobile phase B concentration of 20%. Starting at lower pH was investigated but resulted in insufficient column binding or high run-to-run variability (Fig. S1, ESI†). The developed gradient facilitated the separation of full and empty capsids, represented by the two dominant peaks in each case, as verified later. While AAV5 and 6 seem base line separated, AAV8 shows partial separation, a clear distinction of two discrete peaks is however feasible. It should be mentioned that AAV6 benefitted from separation at higher temperature which significantly improved peak shape and that a comparable improvement was not observed for AAV5 and 8. Based on BLAST alignment searches we were able to conclude that sequence homology alone is not a reliable predictor for the optimum separation temperature. The mobile phases used were of low ionic strength and composed of MS-friendly components only, allowing for subsequent mass spectrometric interfacing if desired. Despite the relatively low ionic strength and limited buffering capacity, full column equilibration was achieved in 12 minutes. A flow rate of 0.2 mL min^{-1} was employed, which allowed for swift column equilibration as well as full

desolvation of the LC effluent in the MS interface in case of mass spectrometric hyphenation. Details describing experimental procedures can be found in the ESI.† After initial method development, the quality of the separations was further investigated. Elution order was determined first by the injection of full and empty material independently, in addition to the mixtures shown in Fig. 1. The resulting chromatograms are depicted in Fig. 2. In pH-gradient AEX a starting mobile phase pH is chosen where all analytes are negatively charged and initially bind to the column. During a gradient from high to low pH, analytes successively elute off the column as the mobile phase pH equals their respective pI's, facilitating separation. In all cases, surprisingly, full capsids were eluting first, which is counterintuitive considering the apparently higher pI of the empty particle and contrary to what is reported in literature for salt-gradient mediated elution.

We propose that the acidic mobile phase pH at the end of the gradient results in a conformational change, thus altering the surface charge distribution of the particles and in consequence their pI. VP 1 was previously reported to undergo structural changes if subjected to heat stress or low pH.[11,27] The N-terminal phospholipase A2 domain of the capsid protein was shown to undergo a reversible unfolding/refolding process at a pH of 5.5–4.0 which leaves the capsid intact. The authors of the study speculated that the underlying mechanism was charge repulsion between the N-terminal domain, internal capsid residues and DNA, which leads to externalization of the phospholipase A2 domain.[11] This process almost certainly triggers changes in the surface charge distribution of the capsid and most likely plays out differently under a complete absence of cargo DNA. It is conceivable that sequence and size of the cargo DNA impact the magnitude of this structural change and that different transgenes could be associated with different retention behaviour in chromatography, which was however not investigated in the current study. Interestingly, full/empty samples showed high variability in their proportions of full and empty capsids, despite being all based on theoretical 1 : 1 mixtures (Fig. 1 and 2, top panel). Calculations of the full-to-empty ratios revealed that samples did not perfectly represent the expected proportions. AAV6 shows the largest discrepancy with the empty particles making up a total of 77.2 instead of 50% of capsids in the sample (Table S1, ESI†). Injections of individual species shown in Fig. 2 (mid and lower panels) clearly demonstrate that the reason is insufficient purity of commercially sourced material, especially the full capsid samples. Analysis-related bias can be ruled out as results obtained for AAV5 were benchmarked against and showed excellent correlation to previously conducted CDMS experiments (Fig. S2, ESI†). In terms of chromatographic performance, it appears that the different capsid fill states of AAV5 are best separated, followed by AAV6 and AAV8. AAV8 moreover shows an increased peak width when compared to serotypes 5 and 6. Calculated chromatographic resolution for each separation supports these findings (Table 1). With an experimentally determined chromatographic resolution of 4.30, AAV5 shows the highest resolution between full and empty capsid peaks followed by AAV6 with a calculated resolution of 2.99. AAV8 is not visibly baseline
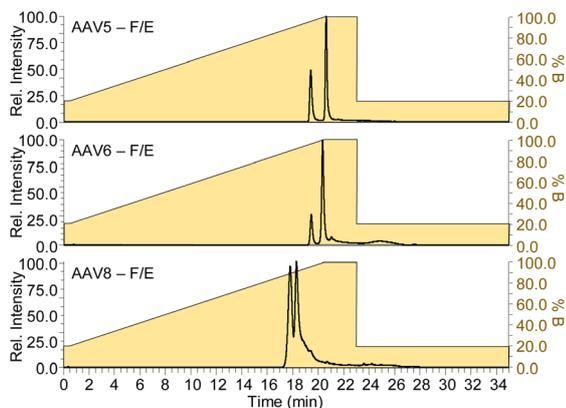

Fig. 1 Separation of AAV5, 6 and 8. The two dominant peaks in each chromatogram represent full and empty capsid species. The mobile phase gradient is indicated in yellow.
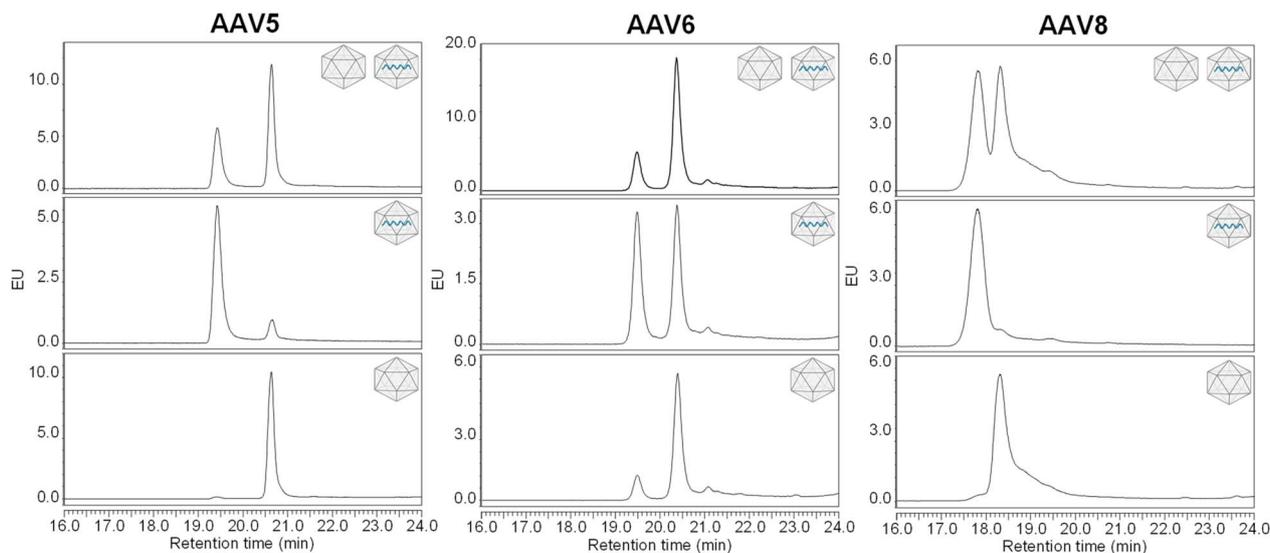
Fig. 2 Chromatograms obtained by AEX of AAV5, 6 and 8 of full and empty capsids as well as of a mixture, respectively. Full capsid samples are indicated by the capsid schematic containing a DNA strand whereas for empty capsid samples the schematic appears empty. For better visualization, only retention time regions of interest are presented.

Table 1 Chromatographic resolution and peak capacity calculated for the full/empty separation of AAV5, 6 and 8. Shown values represent the average of triplicate measurements

Serotype	Resolution	Peak capacity
AAV5	4.30	63.5
AAV6	2.99	56.8
AAV8	1.05	31.6

separated which is reflected by a chromatographic resolution of 1.05. Calculated peak capacities follow the same trend with AAV5 showing a value of 63.5, followed by AAV6 with 56.8 and lastly AAV8 with 31.6, which was expected given the visibly broader peaks.

Also run-to-run variability was evaluated and was found negligible for retention time with relative calculated standard deviations of below 0.1% for full and empty capsid peaks of all three AAVs tested (Table S2, ESI†). Relative standard deviations of peak areas were higher, in a range of 1 to 5%. The largest deviation was observed for AAV6 (4.79%). It should be noted that AAVs are prone to non-specific adsorption to solid surfaces which can occur throughout all stages of production and characterization.[28] Materials that were shown to retain AAV particles include plastics, stainless steel and importantly also glass, the material here used to contain AAV samples in the LC autosampler. Variations in peak area potentially result from adsorption to the HPLC vial, rather than being method related, which is also supported by the observed run-to-run decrease in the fluorescence response, as depicted in Fig. S3 (ESI).† Furthermore, AAVs reportedly experience diluent dependent sample degradation over time, which can be a factor contributing to the variation seen.[32] AAV6 is shown as an example, the fluorescence signal can be seen to slightly decrease from run 1

to 2 and from 2 to 3. Moreover, it appears as if the extent of adsorption is not the same for full and empty species with the full particle peak showing a more pronounced signal loss over time.

After investigation of the chromatographic performance, mass spectrometric interfacing was explored by coupling the separation system to a Thermo Scientific Q Exactive UHMR mass spectrometer with a mass range adequate for the analysis of macromolecules in the megadalton range. While previous investigations show that native mass spectrometry does not reliably facilitate mass determination of AAVs, literature suggests that full and empty particles carry the same extent of positive charges after ionization.[29] Consequently, their MS signals appear in different regions in the m/z domain, depending on whether they carry cargo DNA or not, allowing for their discrimination.[30] Fig. 3a shows the total ion current chromatograms (TICCs) of the three AAV full/empty mixtures corresponding to separations in Fig. 2. Clear MS signals were obtained in all cases with AAV5 and 6 showing good signal intensity while the intensity of AAV8 appeared lower. This was to some extent also observed in fluorescence traces in Fig. 2, likely caused by the increased peak width of that particular serotype.

Other contributing factors could be a higher non-specific adsorption of AAV8 to surfaces or lower MS ionization and ion trapping efficiencies when compared to the other two serotypes investigated. Nonetheless, the MS signal strength allowed for collection of useful mass spectra also for AAV8.

Fig. 3b shows the mass spectra corresponding to peaks in A after peak integration and spectral averaging. In all cases spectra of the earlier eluting peak appeared in a m/z region of around 30 000 while spectra from the later eluting peak were centered at around 22 500 m/z. Assuming a similar molecular charge after MS ionization, the earlier eluting peak must
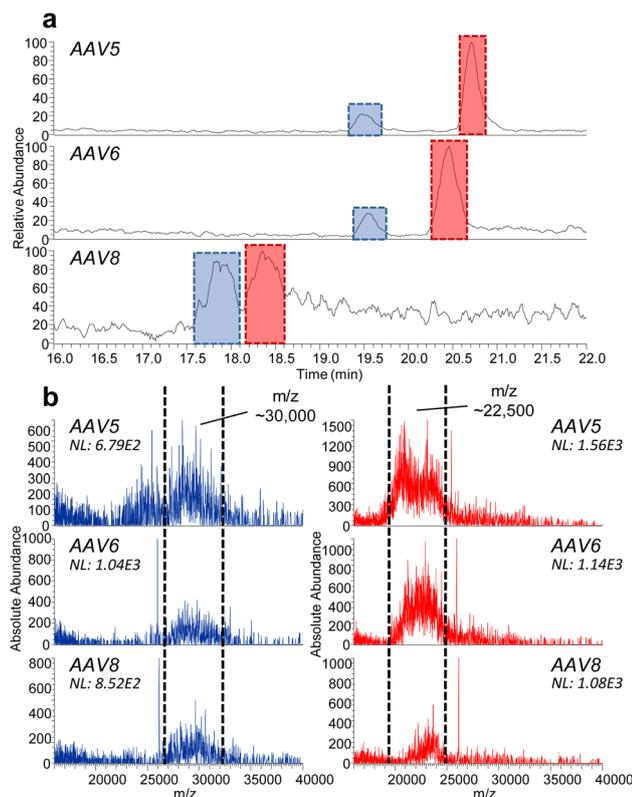
Fig. 3 (a) TICCs corresponding to full/empty fluorescence traces shown in Fig. 2, a magnification of the retention time region of interest is presented. Peaks corresponding to full particles are labelled in blue, peaks corresponding to empty capsids are labelled in red. (b) Associated native mass spectra obtained after integration of peaks labelled in (a). The colour coding is in line with (a).

contain species of significantly higher molecular mass which can of course be explained by the presence of cargo DNA, adding an additional mass of approximately 0.8 MDa. As was already anticipated, the complexity of the samples did not allow for deconvolution and mass determination but indeed for a clear differentiation of full and empty capsids, also confirming the elution order previously determined based on injection of individual full and empty samples (Fig. 2).

The presented method allows for the pH-gradient separation of full and empty capsids of multiple AAV serotypes based on MS-friendly anion exchange chromatography. Fluorescence signals can be utilized to precisely quantify full and empty capsid proportions while subsequent mass spectrometric interfacing allows for peak assignment. Further investigations will be needed to better understand the relationship between AAV structure, including type of the transgene encapsided and retention behaviour. Recently, interfacing of liquid chromatography to CDMS was demonstrated for the first time.[31] While native MS did not allow for precise mass determination and the distinction of possibly present forms other than full and empty species, CDMS might very well be capable of doing so. Whether liquid chromatography in combination with CDMS is feasible for highly heterogeneous macromolecules such as AAVs still needs investigation, but the foundation has been laid

for the development of more sophisticated and informative AAV characterization strategies which are based on liquid chromatography and mass spectrometry.

Author contributions

F. G. was involved in experimental planning, method development and data curation, F. F. was engaged in data curation, data interpretation, illustration and writing of the original manuscript draft, L. S. was engaged in experimental planning, method development and data interpretation. J. B. was involved in experimental planning, project organization and funding acquisition. All authors were engaged in proof-reading of the manuscript draft.

Conflicts of interest

This study was conducted with support of Thermo Fisher Scientific, the company distributing the separation column, analytical instrumentation and data analysis solutions employed in this study. Beyond that, the authors are not aware of any potential conflicts of interest.

Notes and references

1 Y. Gong, A. Berenson, F. Laheji, G. Gao, D. Wang, C. Ng, A. Volak, R. Kok, V. Kreouzis, I. M. Dijkstra, S. Kemp, C. A. Maguire and F. Eichler, *Hum. Gene Ther.*, 2019, **30**, 544–555.
2 L. Samaranch, A. Perez-Canamas, B. Soto-Huelin, V. Sudhakar, J. Jurado-Arjona, P. Hadaczek, J. Avila, J. R. Bringas, J. Casas, H. Chen, X. He, E. H. Schuchman, S. H. Cheng, J. Forsayeth, K. S. Bankiewicz and M. D. Ledesma, *Sci. Transl. Med.*, 2019, **11**, eaat3738.
3 D. Wang, P. W. L. Tai and G. Gao, *Nat. Rev. Drug Discovery*, 2019, **18**, 358–378.
4 S. S. Issa, A. A. Shaimardanova, V. V. Solovyeva and A. A. Rizvanov, *Cells*, 2023, **12**(5), 785.
5 S. Kronenberg, J. A. Kleinschmidt and B. Bottcher, *EMBO Rep.*, 2001, **2**, 997–1002.
6 J. F. Wright, *Biomedicines*, 2014, **2**, 80–97.
7 M. Schnodt and H. Buning, *Hum. Gene Ther. Methods*, 2017, **28**, 101–108.
8 F. Mingozzi, X. M. Anguela, G. Pavani, Y. Chen, R. J. Davidson, D. J. Hui, M. Yazicioglu, L. Elkouby, C. J. Hinderer, A. Faella, C. Howard, A. Tai, G. M. Podsakoff, S. Zhou, E. Basner-Tschakarjan, J. F. Wright and K. A. High, *Sci. Transl. Med.*, 2013, **5**, 194ra192.
9 K. Gao, M. Li, L. Zhong, Q. Su, J. Li, S. Li, R. He, Y. Zhang, G. Hendricks, J. Wang and G. Gao, *Mol. Ther.–Methods Clin. Dev.*, 2014, **1**, 20139.
10 B. Burnham, S. Nass, E. Kong, M. Mattingly, D. Woodcock, A. Song, S. Wadsworth, S. H. Cheng, A. Scaria and C. R. O'Riordan, *Hum. Gene Ther. Methods*, 2015, **26**, 228–242.

11 B. Venkatakrishnan, J. Yarbrough, J. Domsic, A. Bennett, B. Bothner, O. G. Kozyreva, R. J. Samulski, N. Muzyczka, R. McKenna and M. Agbandje-McKenna, *J. Virol.*, 2013, **87**, 4974–4984.

12 M. Urabe, K. Q. Xin, Y. Obara, T. Nakakura, H. Mizukami, A. Kume, K. Okuda and K. Ozawa, *Mol. Ther.*, 2006, **13**, 823–828.

13 N. Kaludov, B. Handelman and J. A. Chiorini, *Hum. Gene Ther.*, 2002, **13**, 1235–1243.

14 G. Qu, J. Bahr-Davidson, J. Prado, A. Tai, F. Cataniag, J. McDonnell, J. Zhou, B. Hauck, J. Luna, J. M. Sommer, P. Smith, S. Zhou, P. Colosi, K. A. High, G. F. Pierce and J. F. Wright, *J. Virol. Methods*, 2007, **140**, 183–192.

15 C. Wang, S. H. R. Mulagapati, Z. Chen, J. Du, X. Zhao, G. Xi, L. Chen, T. Linke, C. Gao, A. E. Schmelzer and D. Liu, *Mol. Ther.–Methods Clin. Dev.*, 2019, **15**, 257–263.

16 M. Lock, M. R. Alvira and J. M. Wilson, *Hum. Gene Ther. Methods*, 2012, **23**, 56–64.

17 S. L. Khatwani, A. Pavlova and Z. Pirot, *Mol. Ther.–Methods Clin. Dev.*, 2021, **21**, 548–558.

18 S. Fekete, M. K. Aebischer, M. Imiolek, T. Graf, R. Ruppert, M. Lauber, V. D'Atri and D. Guillarme, *Trends Anal. Chem.*, 2023, **164**, 117088.

19 K. Richter, C. Wurm, K. Strasser, J. Bauer, M. Bakou, R. VerHeul, S. Sternisha, A. Hawe, M. Salomon, T. Menzen and A. Bhattacharya, *Eur. J. Pharm. Biopharm.*, 2023, **189**, 68–83.

20 C. Wagner, F. F. Fuchsberger, B. Innthaler, M. Lemmerer and R. Birner-Gruenberger, *Int. J. Mol. Sci.*, 2023, **24**, 11033.

21 E. Ebberink, A. Ruisinger, M. Nuebel, M. Thomann and A. J. R. Heck, *Mol. Ther.–Methods Clin. Dev.*, 2022, **27**, 491–501.

22 T. P. Worner, J. Snijder, O. Friese, T. Powers and A. J. R. Heck, *Mol. Ther.–Methods Clin. Dev.*, 2022, **24**, 40–47.

23 E. E. Pierson, D. Z. Keifer, A. Asokan and M. F. Jarrold, *Anal. Chem.*, 2016, **88**, 6718–6725.

24 F. Fussl, S. Millan-Martin, J. Bones and S. Carillo, *J. Pharm. Biomed. Anal.*, 2023, **234**, 115534.

25 F. Fussl, K. Cook, K. Scheffler, A. Farrell, S. Mittermayr and J. Bones, *Anal. Chem.*, 2018, **90**, 4669–4676.

26 F. Fussl, A. Criscuolo, K. Cook, K. Scheffler and J. Bones, *J. Proteome Res.*, 2019, **18**, 3689–3702.

27 S. Kronenberg, B. Bottcher, C. W. von der Lieth, S. Bleker and J. A. Kleinschmidt, *J. Virol.*, 2005, **79**, 5296–5303.

28 S. Ramy, Y. Ueda, H. Nakajima, Y. Hiroi, T. Torisu and S. Uchiyama, *J. Pharm. Sci.*, 2022, **111**, 663–671.

29 T. P. Worner, J. Snijder, A. Bennett, M. Agbandje-McKenna, A. A. Makarov and A. J. R. Heck, *Nat. Methods*, 2020, **17**, 395–398.

30 L. Strasser, T. E. Morgan, F. Guapo, F. Fussl, D. Forsey, I. Anderson and J. Bones, *Anal. Chem.*, 2021, **93**, 12817–12821.

31 L. Strasser, F. Fussl, T. E. Morgan, S. Carillo and J. Bones, *Anal. Chem.*, 2023, **95**, 15118–15124.

32 M. K. Aebischer, H. Gizardin-Fredon, H. Lardeux, D. Kochardt, C. Elger, M. Haindl, R. Ruppert, D. Guillarme and V. D'Atri, *Int. J. Mol. Sci.*, 2022, **23**, 12332.